BEAM DIAGNOSTICS FOR MEDICAL ACCELERATORS

Tomasz Cybulski

University of Liverpool , UK
The Cockcroft Institute, UK

t.cybulski@liv.ac.uk

OUTLINE

- **In**toroduction **to r**adiotherapy
- **Sc**anditronix MC-**60** PF Cyclotron
- A **Q**uality **C**ontrol **T**easer
- **F**araday **C**up **O**ptimisation
- **L**HCb **V**ELO **D**etector
- **Sum**mary

INTRODUCTION TO RADIOTHERAPY


- X – ray photon

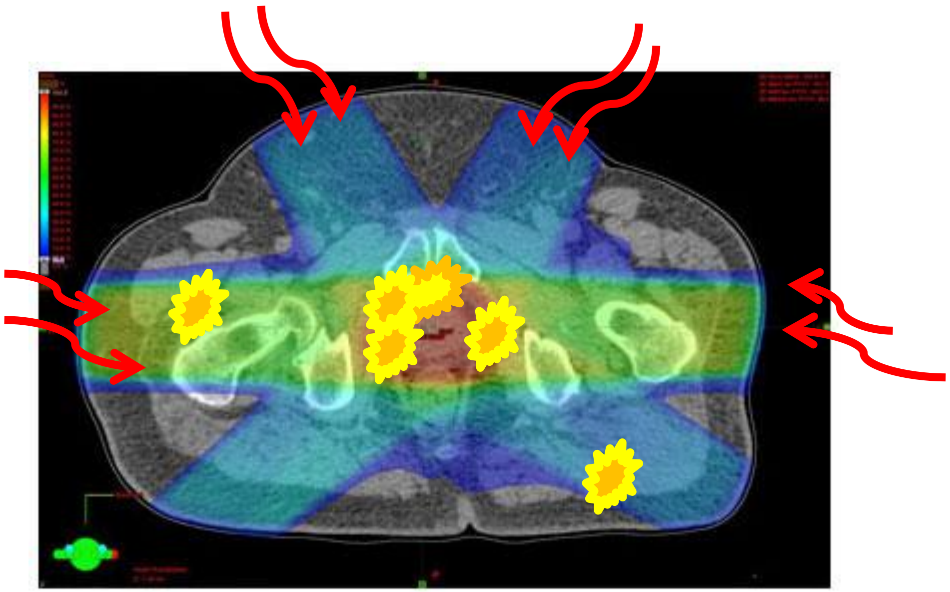

Fig. 1. Principles of conformal radiotherapy. [1]

Fig. 2. Single strand DNA brake. [2]

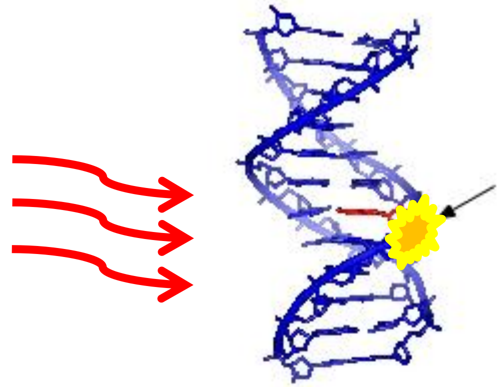

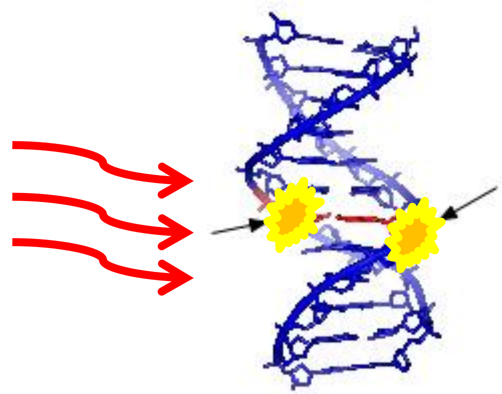

Fig. 3. Double strand DNA brake. [2]

INTRODUCTION TO RADIOTHERAPY

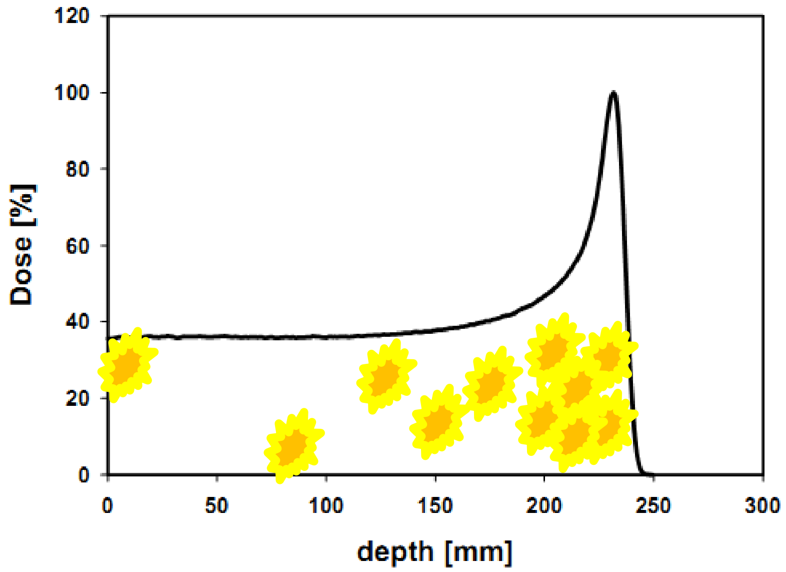

Fig. 4. Energy deposition by proton beam as a function of depth - Bragg peak. [4]

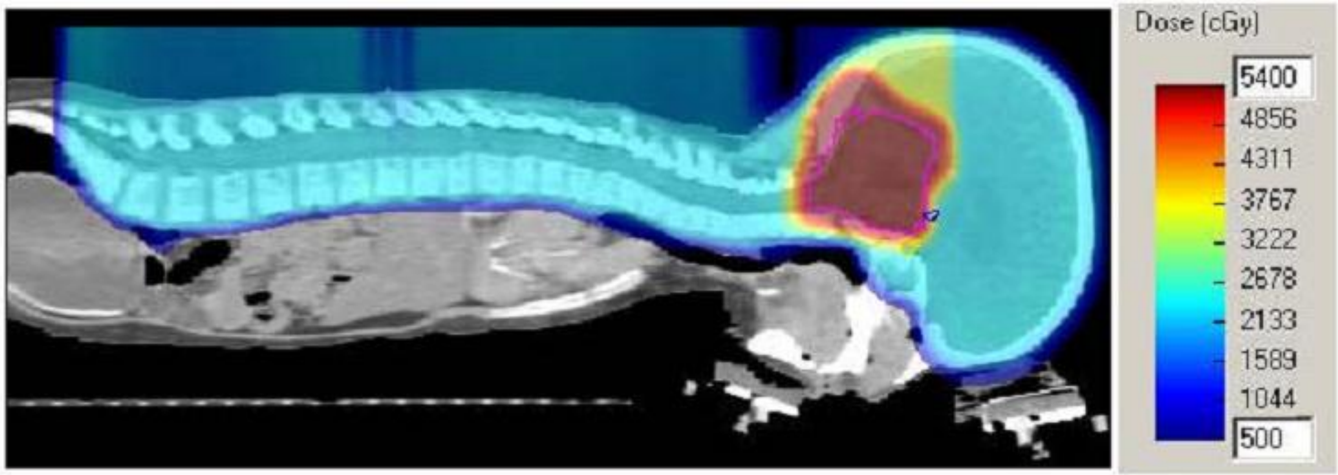

Fig. 6. Sagittal colour-wash dose display for the treatment on meduloblastoma. [4]

INTRODUCTION TO RADIOTHERAPY

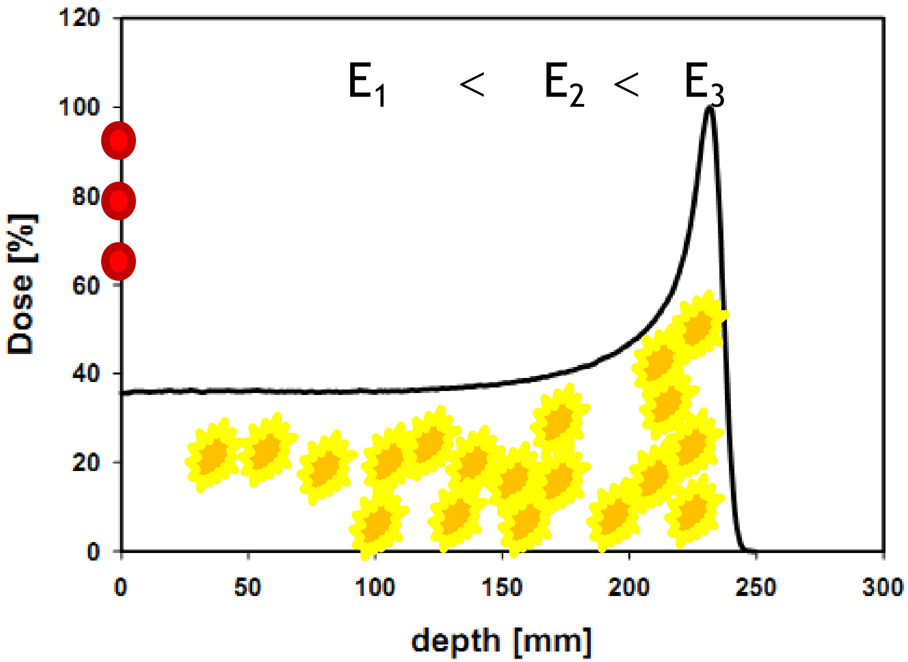

Parameters determining the quality and effectiveness of radiotherapy treatment:

1. **DOSE** – determines energy deposited in a target (tumour) volume – number of ionisation events

   Parameter of importance: **Beam current**

2. **Tumour coverage** – irradiation of tumour volume and protection of healthy tissue

- **Penetration depth** - determines distal tumour coverage
  Parameter of importance: **Energy**
- **Lateral spread** – determines accuracy of lateral irradiation accuracy

SCANDITRONIX MC-60 PF CYCLOTRON

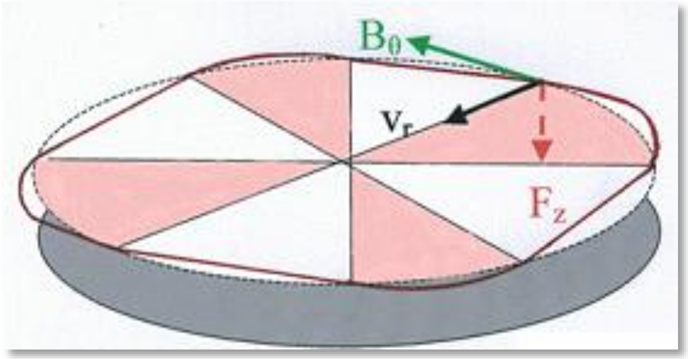

Fig. 6. Scanditronix MC-60 cyclotron is an isochronous machine. Magnetic field corrects the relativistic mass effect: $m = \gamma \cdot m_0$, to hold the synchronism

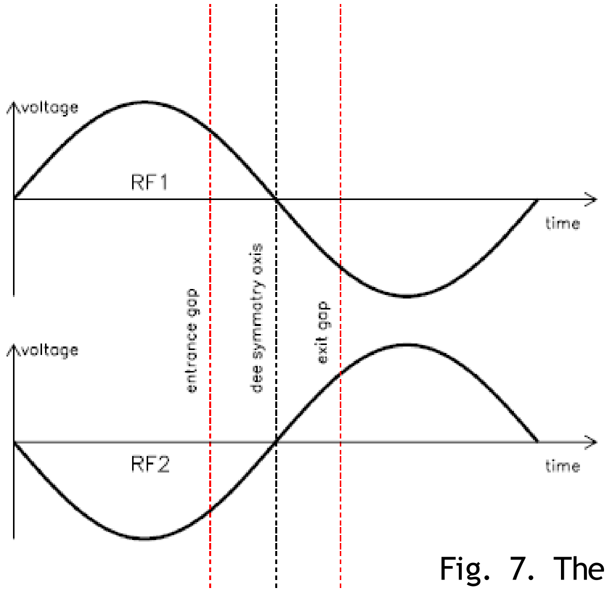

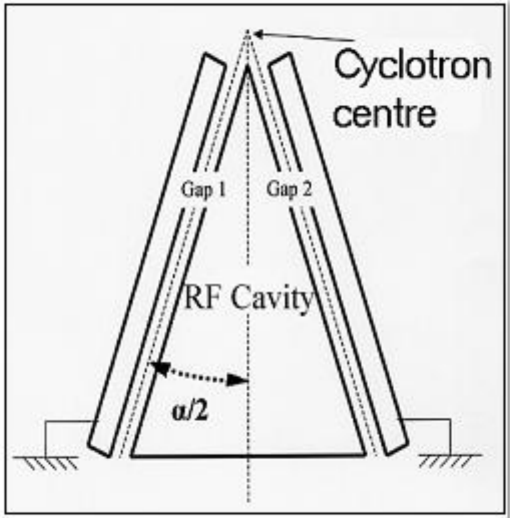

Fig. 7. The RF acceleration takes place in RF cavities of the width of 90 RF degrees. The RF pull push method is used.

IntRo
SC60
QCT
FCO
LHCb
Sum

SCANDITRONIX MC-60 PF CYCLOTRON

Scanditronix MC – 60 Cyclotron characteristics	
Ions	p
Energy [MeV]	62
PIG source max current [mA]	1
Acceleration method	RF
Harmonic modes	1
RF frequency [MHz]	25,7

$$N_{ions} = I_{source} \cdot N_I \cdot \frac{RF\ acceleration\ acceptnace}{360} \cdot \frac{1}{f_{RF}}$$

$$= 8.44\ e + 6$$

$$P = \frac{A}{\zeta} \cdot \frac{i}{e} \cdot W$$

where:
P - beam power [W]
A - mass number of the ion
ζ - charge of the ion
e - 1,602 [As] - ‘the charge in 1 A’
W - kinetic energy of the ions [eV/u]

Therapeutical beam characteristics	
RF period [ns]	37.45
Bunch length [ns]	1.35
Beam current [nA]	5.0
Number of ions per sec.	3.12 e+10
Number of ions per bunch	1.17 e+3
Beam power [W]	3.0 e-1

SCANDITRONIX MC-60 PF CYCLOTRON

The treatment line passive scattering device based on double – W foil scattering .

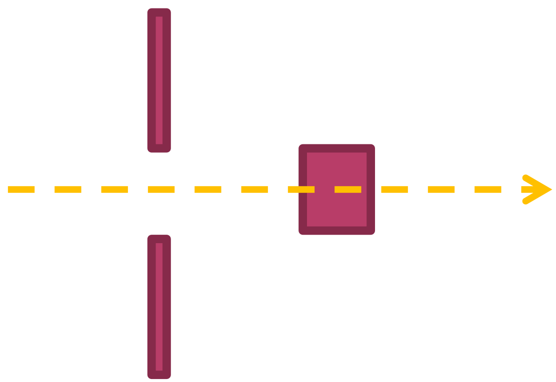

Fig. 8.a. Double - W scattering foils. The thickness is of 20µm is a compromise between the beam lateral spread and energy loss.

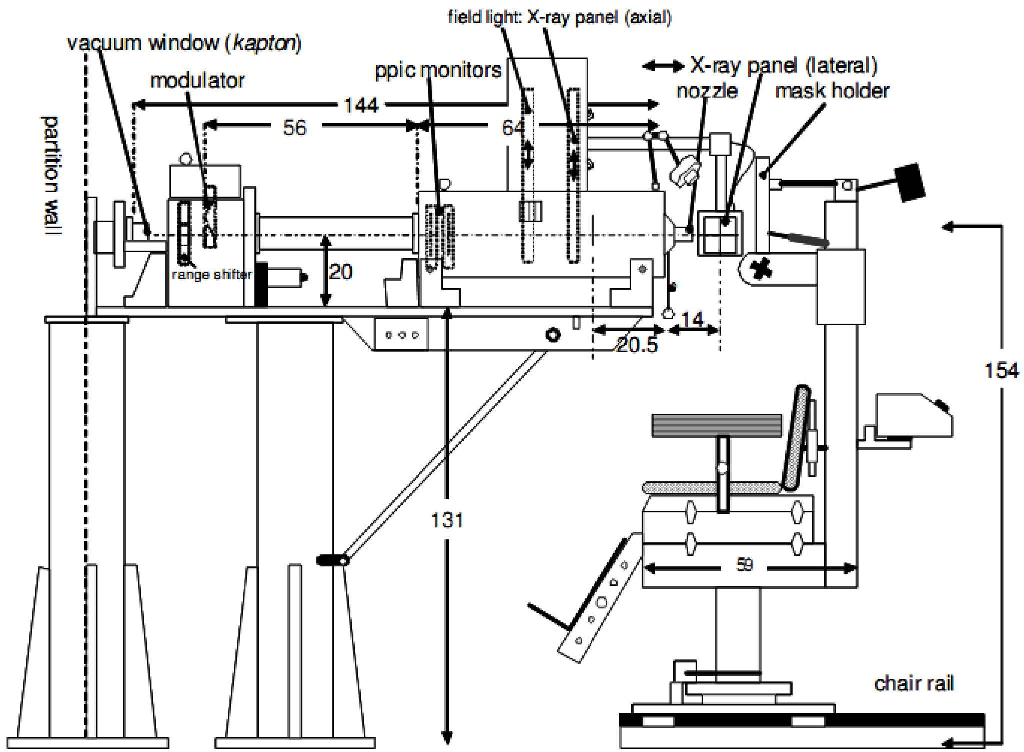

Fig. 8.b. Treatment beam line technical drawing.

A QUALITY CONTROL TEASER

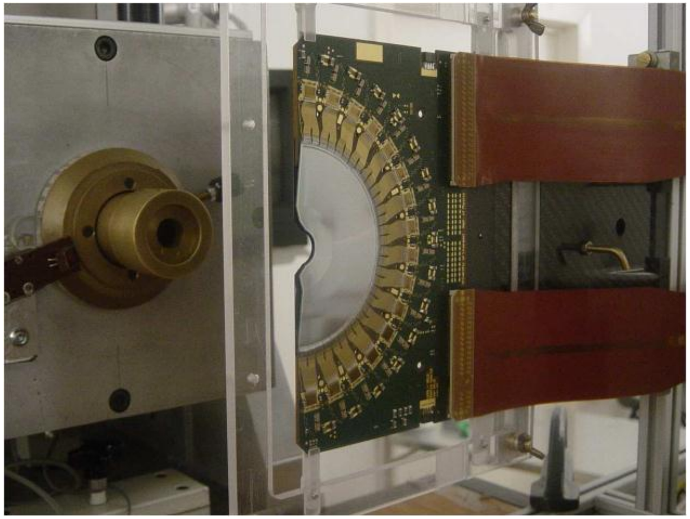

Fig. 9. LHCb VELO module at the Clatterbridge Centre for Oncology. [5]

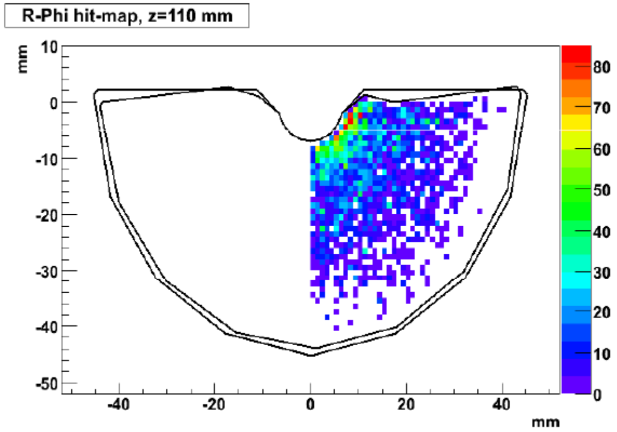

Fig. 10. Beam halo hit map on the LHCb VELO at the distance d = 110 mm from the collimator. [5]

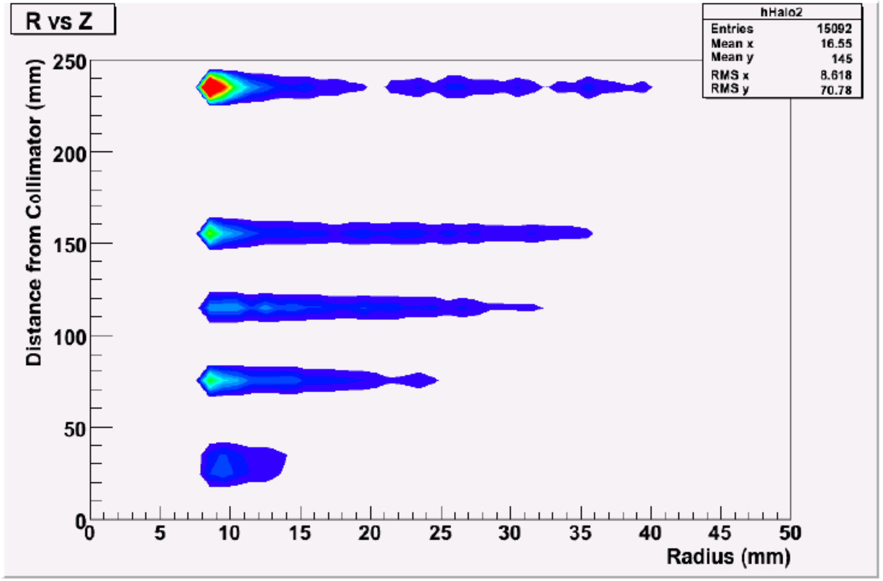

Fig. 11. Divergence of the beam halo as a function of distance from the collimator. [5]

QUALITY CONTROL FOR MEDICAL ACCELERATOR

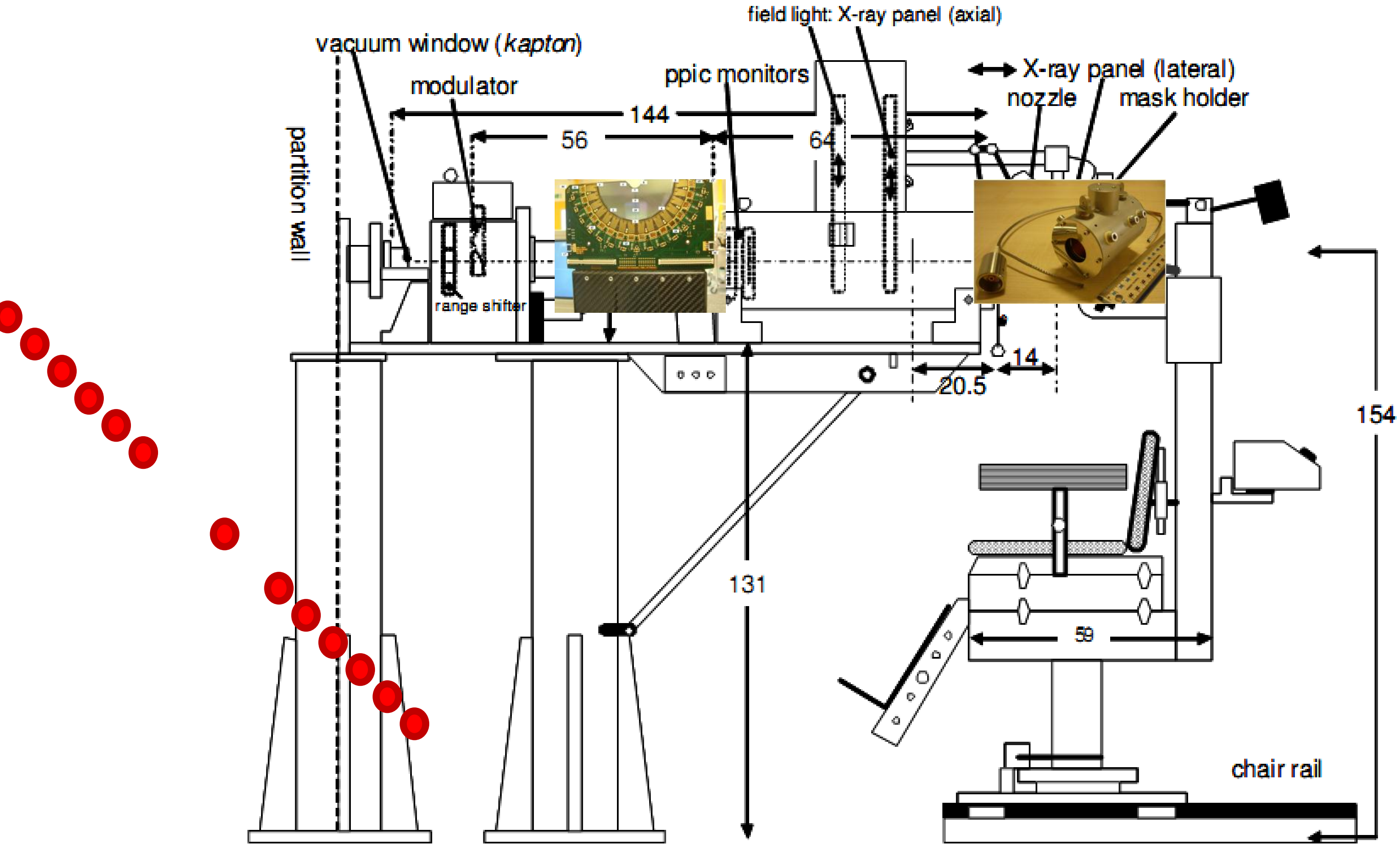

Fig. 12. Treatment room set up at Clatterbridge Centre for Oncology. [3]

IntRo
SC60
QCT
FCO
LHCb
Sum

FARADAY CUP OPTIMISATION

FLUKA – a multi particle transport code – has been used to simulate the optimum geometry for the Faraday CUP design.

FC design requirements:

1. Thickness: enough to stop both primary and secondary particles
2. Depth: enough to make the escaping secondary electrons opening angle as small as possible
3. Material: good electrical conductivity, nuclear reactions have to be considered.
4. Vacuum good enough to avoid ionisation of the residual gas – up to 10^{-5} hPa.

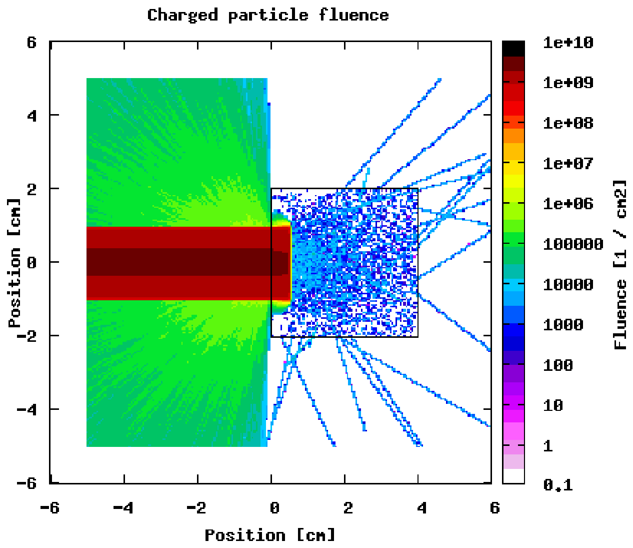

Fig. 13. FLUKA simulation of the 60MeV proton beam impinging on a cubical Cu target. Charged Hadron fluence is estimated for 3.12e10 primary protons.

FARADAY CUP OPTIMISATION

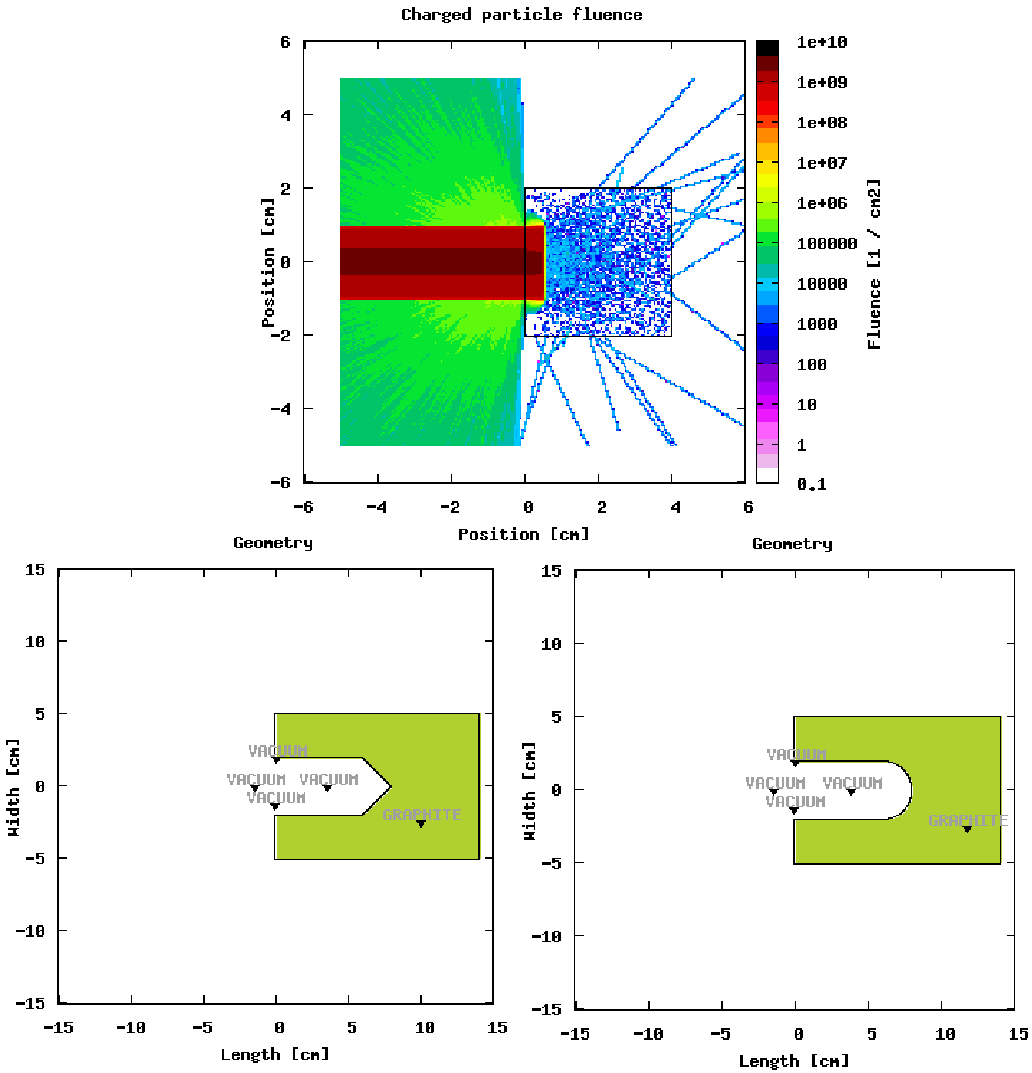

Fig. 14. Geometrical design concept of Faraday Cup.

Tab. 3. Faraday CUP design dimensions. The beam diameter is 2cm.

Aperture Diameter [cm]	4.0
Outer diameter [cm]	8.0
Well length [cm]	4.0
Aperture polar angle [deg]	30
Target thickness [cm]	4.0
Target materials	Copper Aluminum Graphite

IntRo
SC60
QCT
FCO
LHCb
Sum

FARADAY CUP OPTIMISATION

FLUKA input file configuration:

1. Multiple Coulomb Scattering option enabled

2. Electromagnetic FLUKA: production cut for electrons and positrons – 1keV, production cut for photons 0.1keV

3. Electromagnetic interactions thresholds: as for the electromagnetic

4. Secondary proton production threshold: 10^{-6} GeV.

5. Self-shielding option for neutrons enabled (bulky materials may act as „neutron sink” due to neutron resonances)

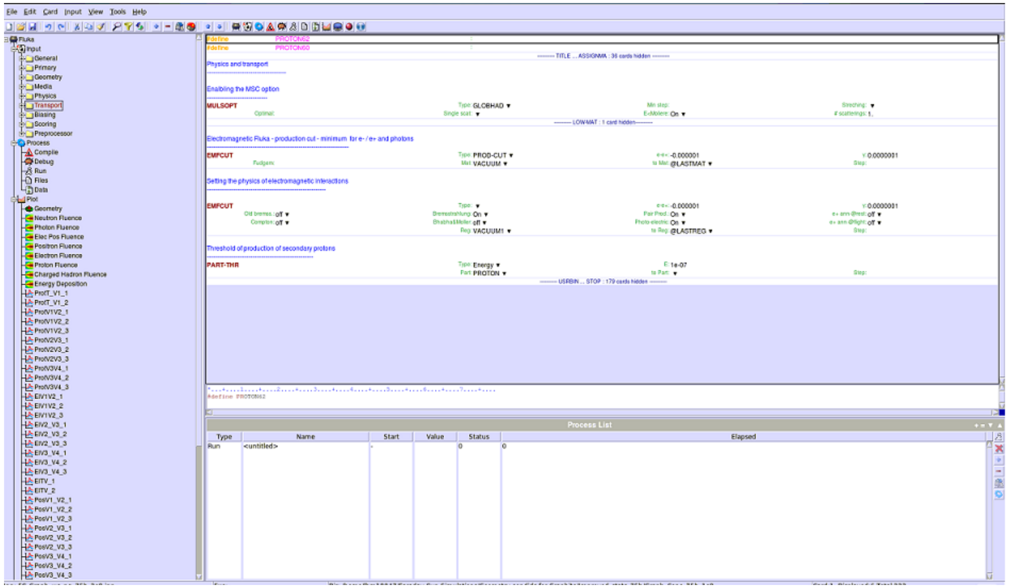

Fig. 14. FAIR interface for the FLUKA simulations.

FARADAY CUP OPTIMISATION

Secondary emission particles spectra simulated for the optimisation of the Faraday CUP:

1. Protons
2. Electrons
3. Positrons
4. Charged particles

Auxiliary simulations:

1. Bremsstrahlung and photons
2. Neutrons flux

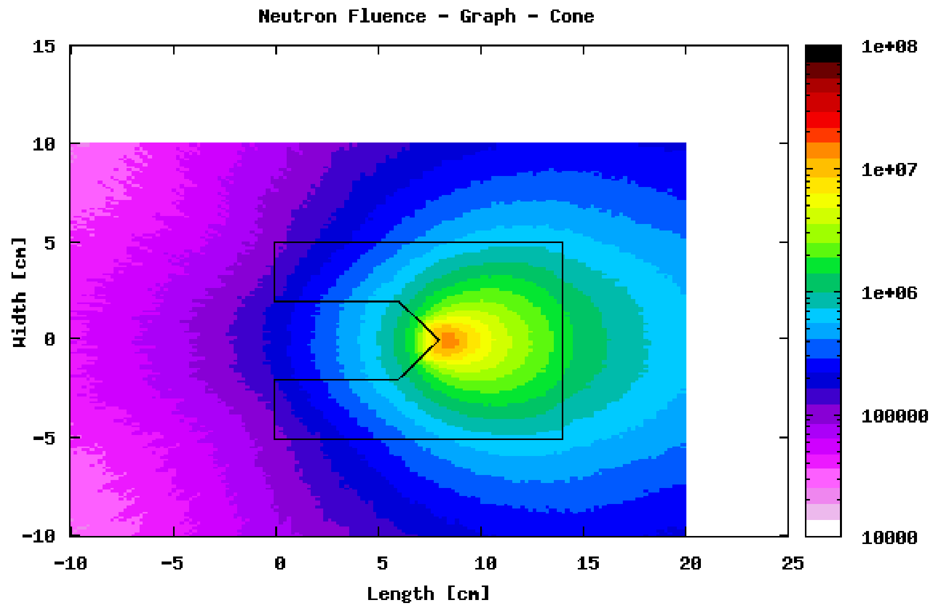

Fig. 15. Neutron fluence for Graphite target – 60MeV proton beam for 3.12e10 particles

- Pions and mions < proton energy lower than production threshold energy (290MeV)

IntRo
SC60
QCT
FCO
LHCb
Sum

FARADAY CUP OPTIMISATION

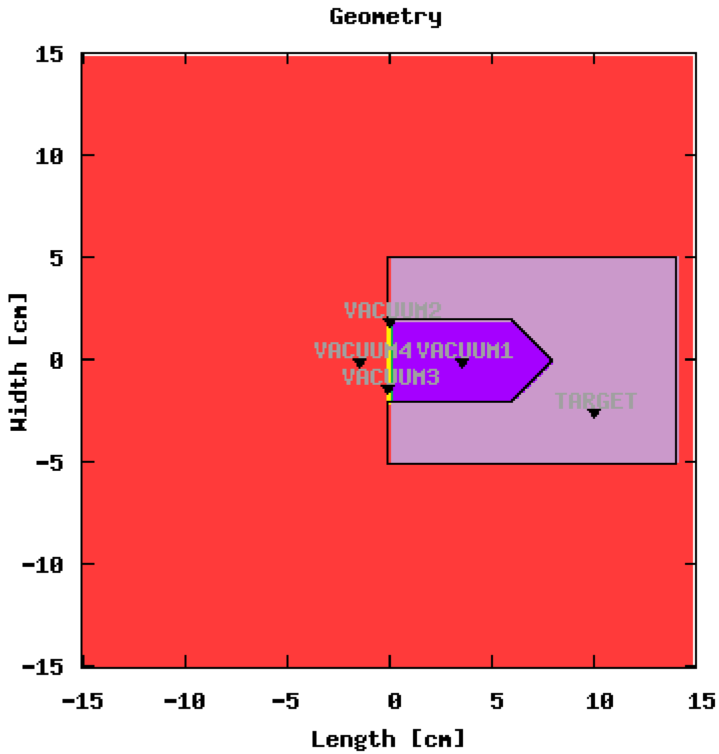

Fig. 16. Regions setup for particles fluence estimation.

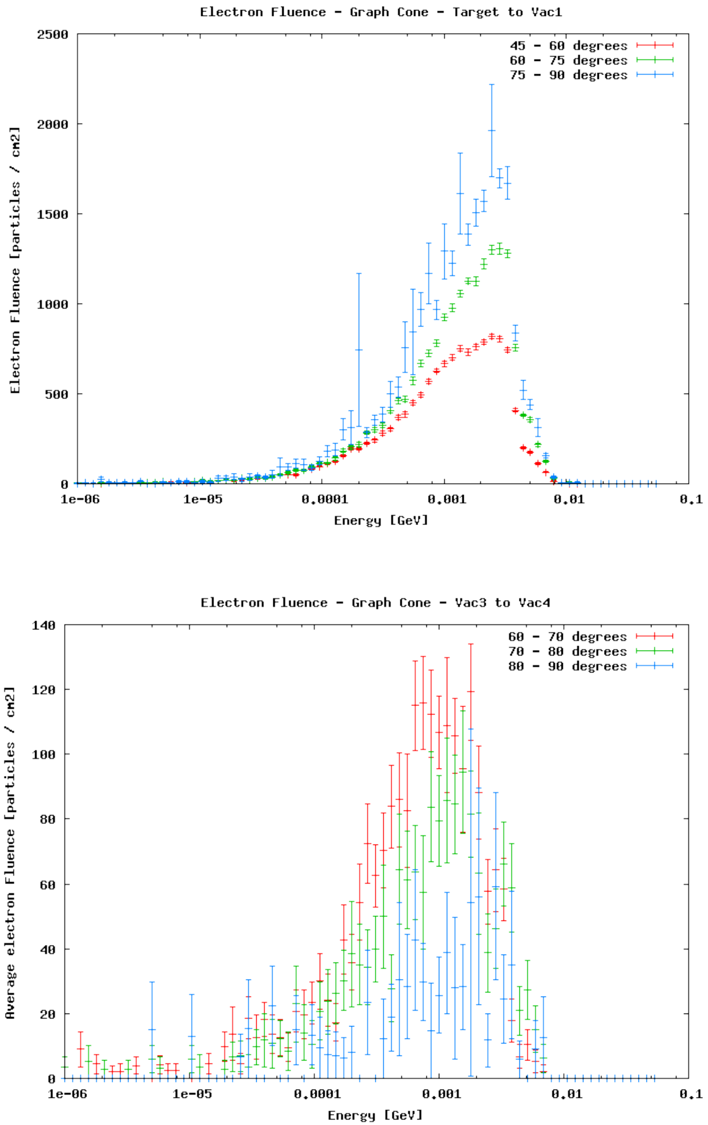

Fig. 19. Electron fluence estimated with the USRDBX estimator (Graphite target). Upper plot – target to Vacuum 1; lower: Vacuum 3 to Vacuum 4.

FARADAY CUP OPTIMISATION

Statistics problem:

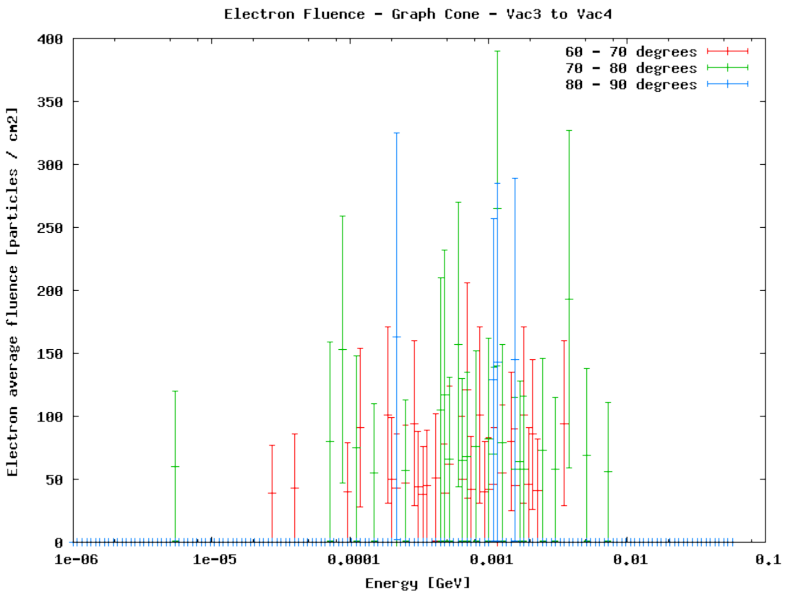

Fig. 17. Simulation results for Graphite target: 75 energy bins, 1e8 protons. (Simulation time for Cu target – 30 days)

Fig. 18. Simulation results for Graphite target: 150 energy bins, 1e6 protons.

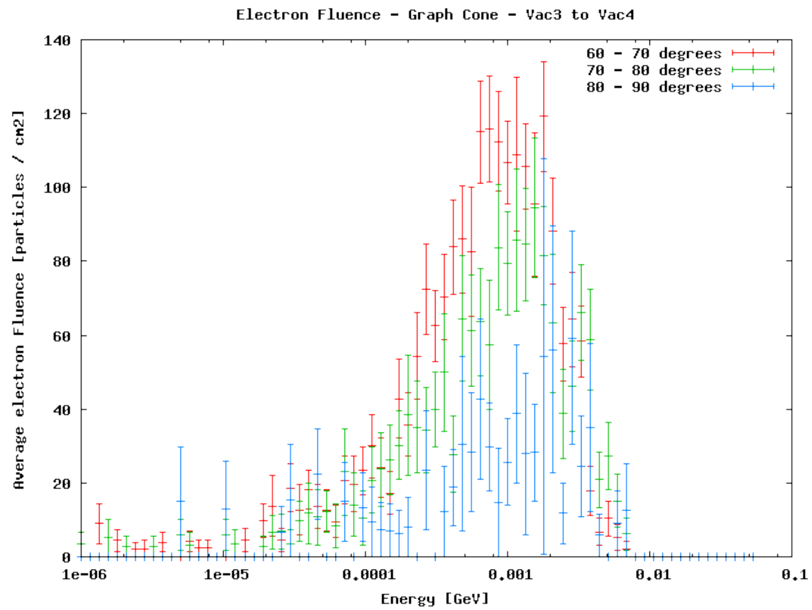

FARADAY CUP OPTIMISATION

Faraday Cup summary:

1. Measurement of 5 nA beam current, the beam stability 5% (0.25nA). The expected measurement sensitivity: maximum 0.01nA

2. Detailed material and geometry investigation will be introduced on completing the simulations

3. Operation time constraints due to thermal effects will be investigated

LHCB VELO DETECTOR

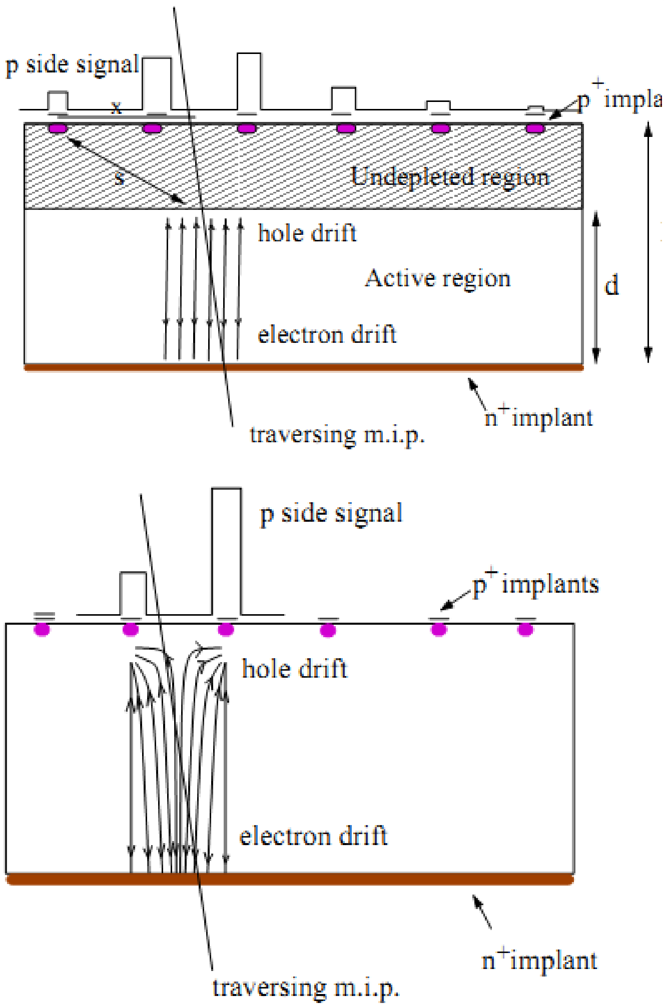

Fig. 19. Cluster shapes for a underdepleted and fully depleted silicon strip detector. [6]

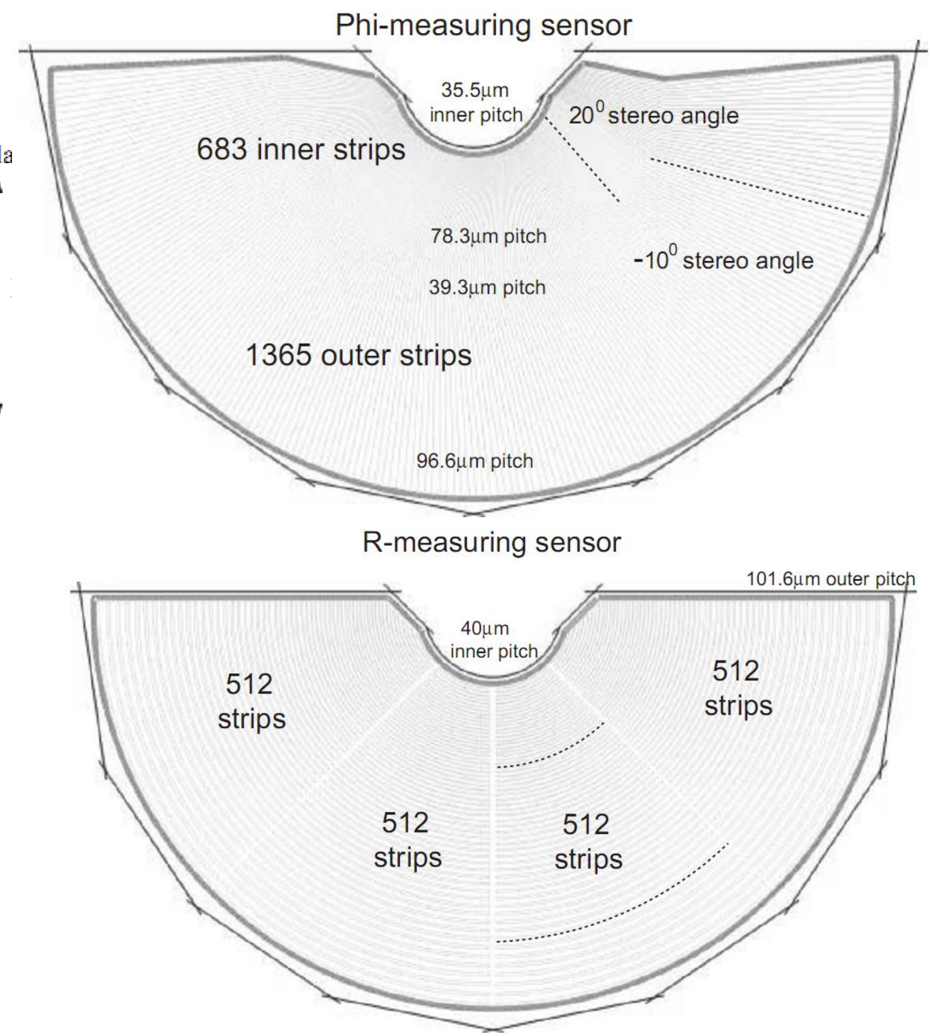

Fig. 20. TDR LHCb VELO detector sensor structure. [6]

LHCB VELO DETECTOR

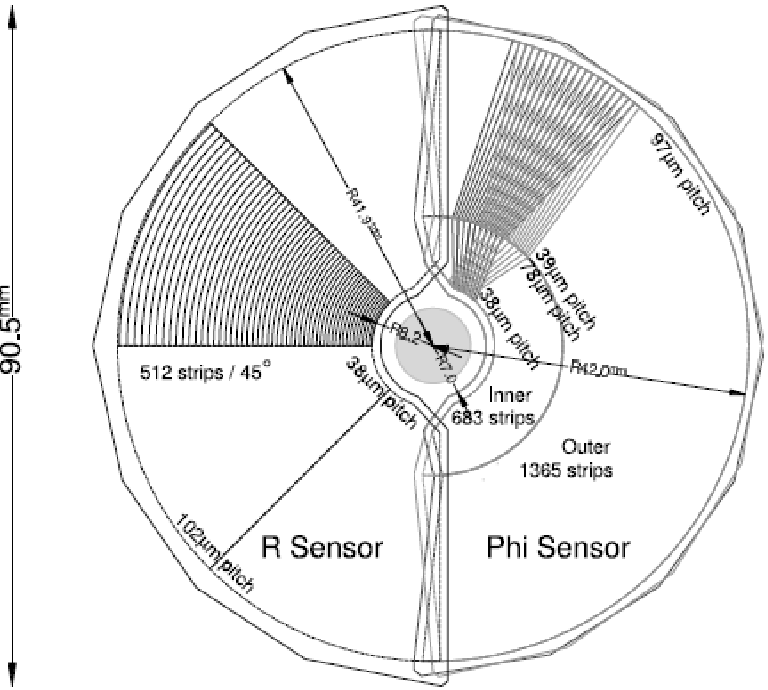

Fig. 21. rφ geometry of the LHCb VELO sensors (n-on-n).

Tab. 4. LHCb VELO sensors parameters

	R sensor	ϕ-sensor
number of sensors	42 + 4 (VETO)	42
readout channels per sensor	2048	2048
sensor thickness	300 μm	300 μm
smallest pitch	40 μm	38 μm
largest pitch	102 μm	97 μm
length of shortest strip	3.8 mm	5.9 mm
length of longest strip	33.8 mm	24.9 mm
inner radius of active area	8.2 mm	8.2 mm
outer radius of active area	42 mm	42 mm
angular coverage	182 deg	$\approx$ 182 deg
stereo angle	-	10–20 deg
double metal layer	yes	yes
average occupancy	1.1%	1.1/0.7% inner/outer

R – sensor strip pitch

$$40 + (101.6 - 40)\,\frac{r - 8190}{41949 - 8190}$$

φ – sensor strip pitch

$$37.7 + (79.5 - 37.7)\,\frac{r - 8170}{17250 - 8170}$$

$$37.7 + (79.5 - 37.7)\,\frac{r - 17250}{42000 - 17250}$$

IntRo ○
SC60 ○
QCT ○
FCO ○
LHCb ●
Sum ○

LHCB VELO DETECTOR

Beetle chip

CMOS technology, 0.12 µm, radiation hard ASIC, analogue

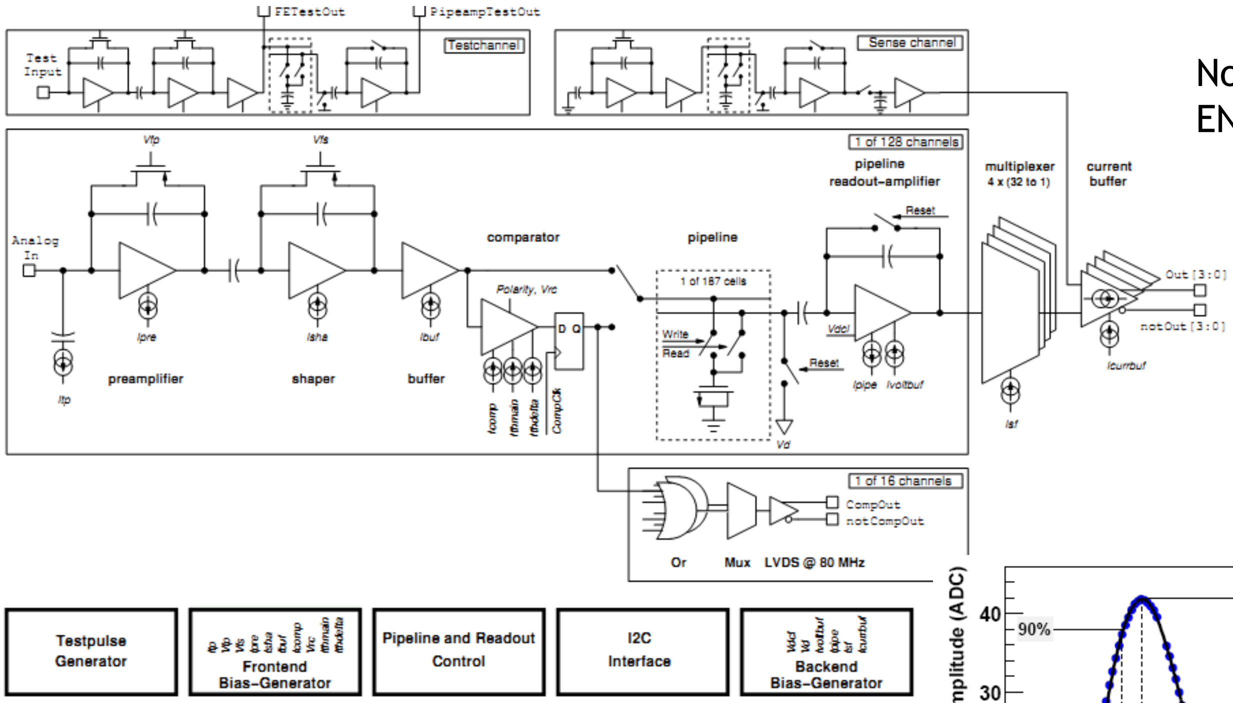

Noise Equivalent Charge
ENC = 790e +17.5e /pF

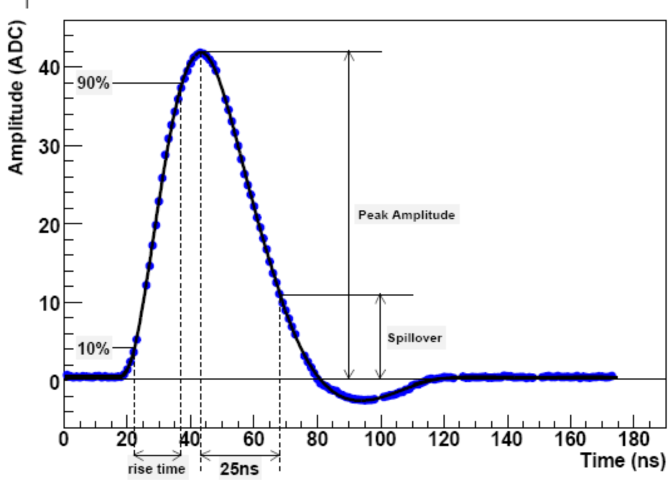

Fig. 22. Beetle chip architecture and pulse shape. The Spill over has to be lower than 0.3 of the peak value after 25ns.[8] The Response of the Beetle to the test-pulse: the measured rise time is 14.7 +/- 0.5 ns and the spill-over (26 +/- 0.6%).

LHCB VELO DETECTOR

LHCb VErtex LOcator (VELO) – reconstruction of vertices tracks of decays of beauty- and charm- hadrons in LHCb experiment.

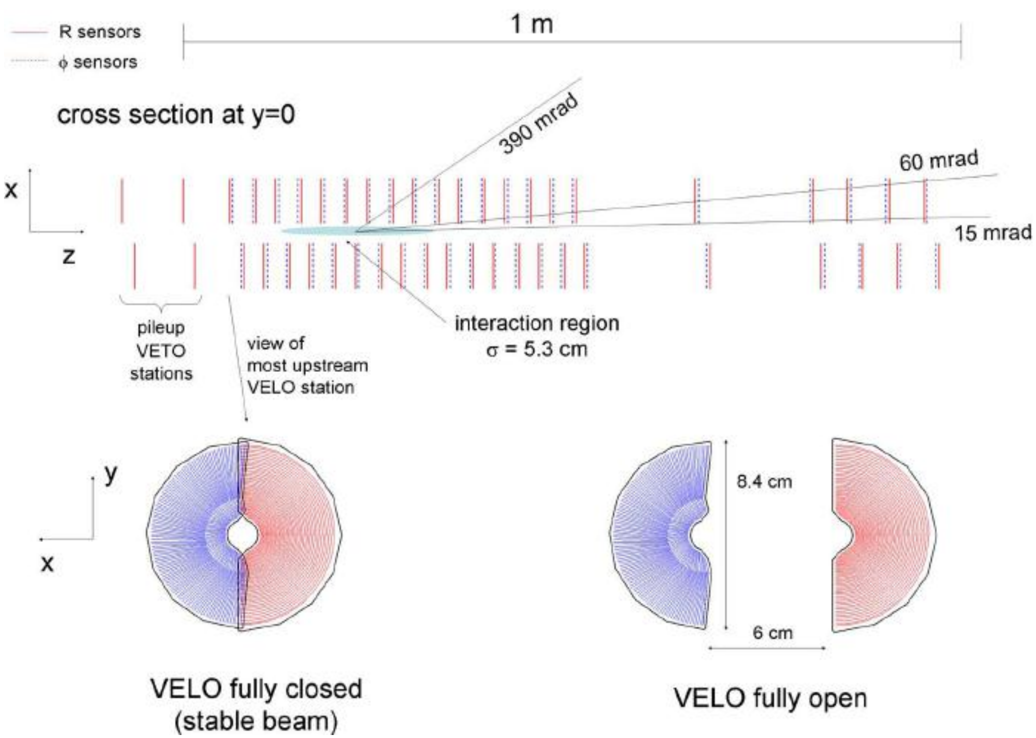

Fig. 23. LHCb VELO modules in cross section in LHCb experiment. [7]

Detector design and construction requirements:

- Performance
- Geometrical
- Environmental
- Machine integration

LHCB VELO ARCHITECTURE

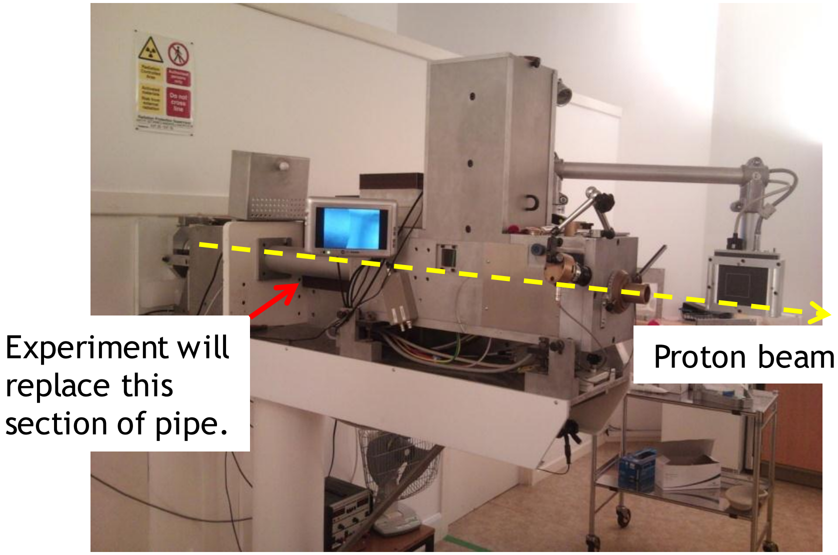

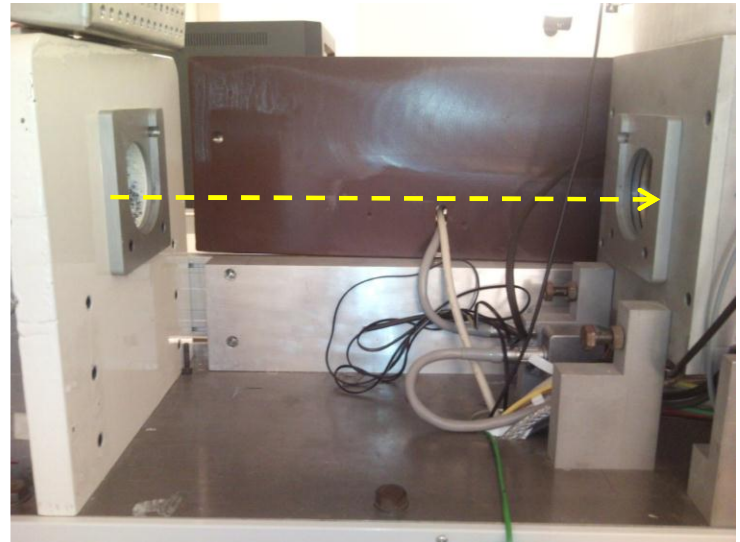

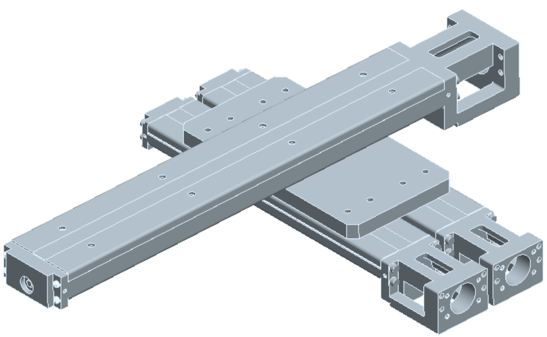

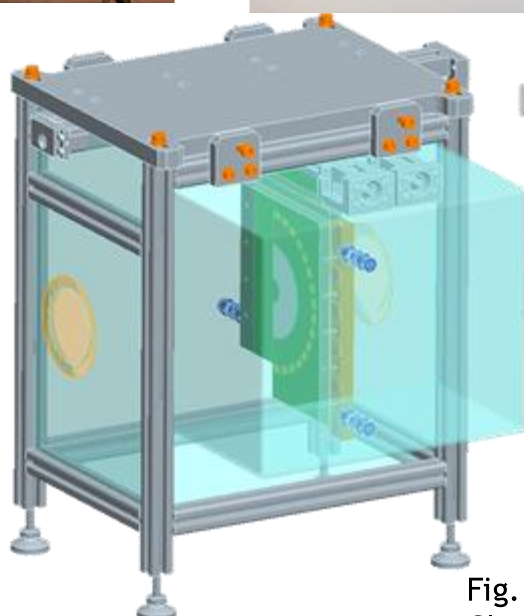

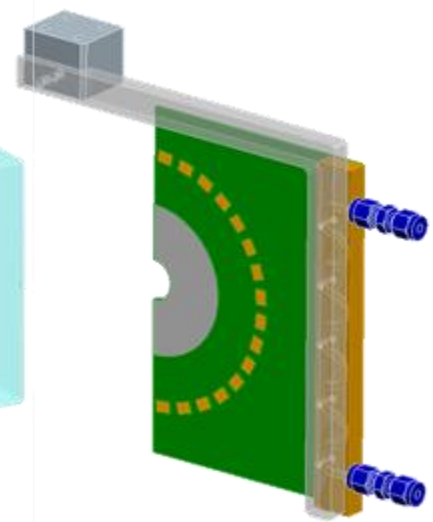

Fig. 24. LHCb VELO stand at the Clatterbridge Centre for Oncology.

LHCB VELO ELECTRONICS

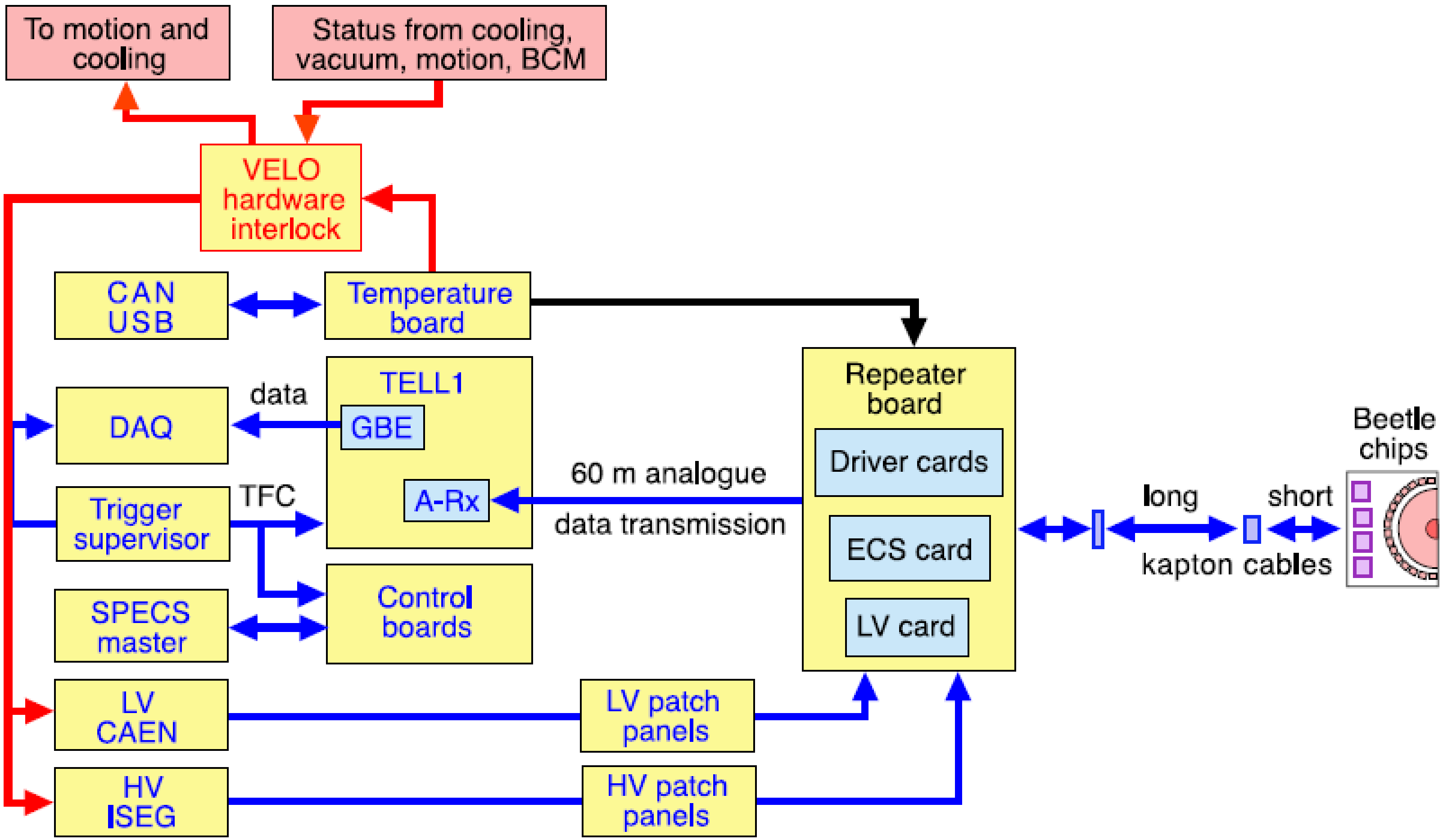

Fig. 25. LHCb VELO readout electronics. [7]

IntRo
SC60
QCT
FCO
LHCb
Sum

LHCB VELO ELECTRONICS

TELL 1 cards for VELO

Functions:

1. Digitization of the data – 10 bit digitizers sample at the frequency of 40 MHz: 4 A-Rx cards, 16 channels each card

2. Pedestal subtraction

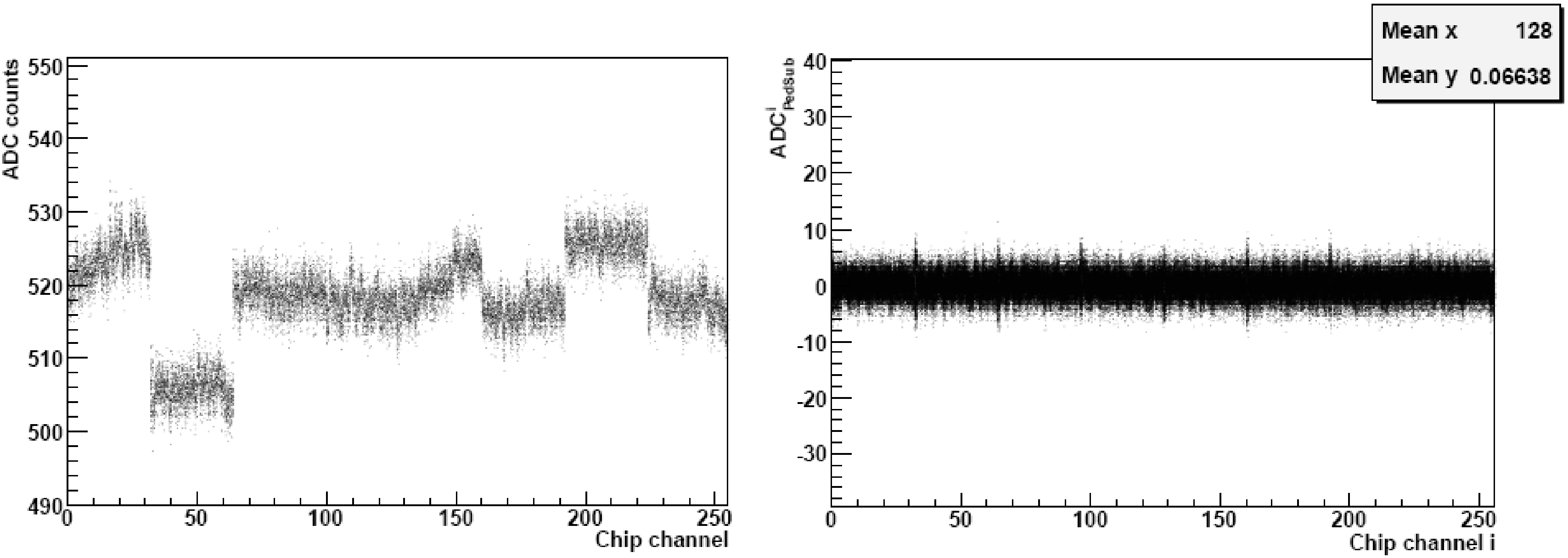

Fig. 26. Pedestal subtraction from the signal determined for two chips. The ADC count corresponds to the charge of approx. 450 electrons, thus the signal is of about 50 ADC counts. The noise is of about 2 – 3 ADC counts. [9]

LHCB VELO DETECTOR

2. Cross – talk removal

3. Channel re-ordering

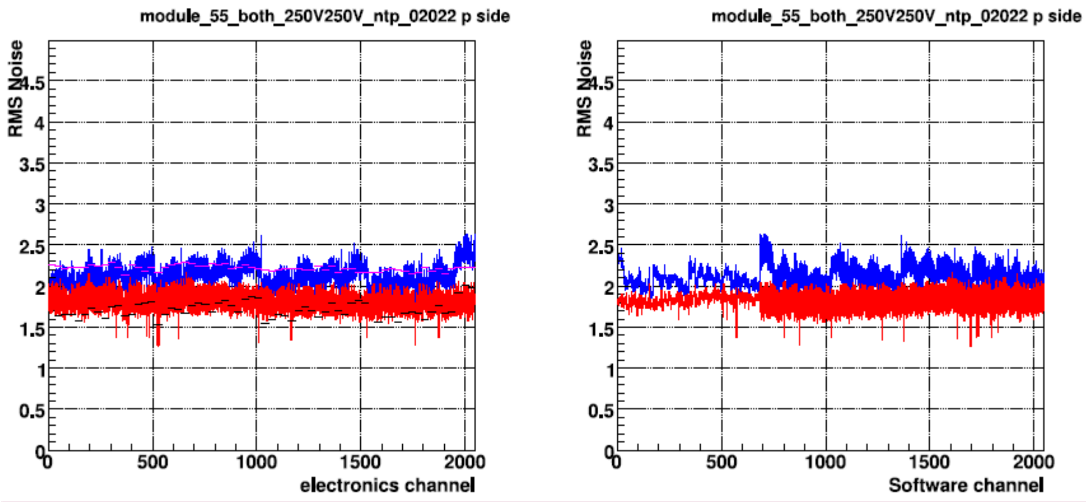

Fig. 27. ADC noise before and after channel reordering in Phi – sensor. [9]

4. Common mode suppression

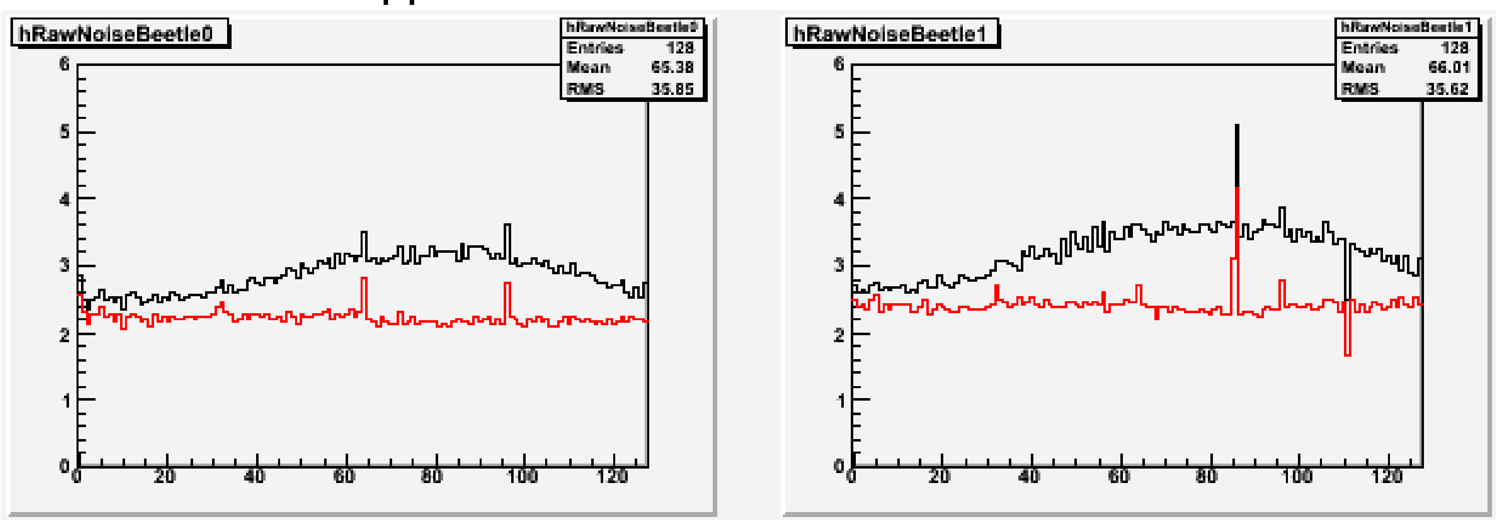

Fig. 28. Common noise suppression for signal from each Beetle Chip.

5. Clustering – up to four strips: seeding treshold, inclusion treshold cut.

BEAM DIAGNOSTICS - SUMMARY

Summary

1. Proof of principle measurements indicate that the LHCb VELO is capable to measure proton beams

2. It seems possible to qualitatively estimate the proton beam halo divergence by use of the VELO detector

3. Further studies will investigate into potential correlations between beam current (Faraday CUP) and halo signal (LHCb VELO)

4. The possible use of the VELO detector as a non-invasive method for beam QC will be assessed

5. A concept of the Multilayer Faraday Cup for beam energy and energy spread will be considered based on classical FC simulations followed by MLFC dedicated studies

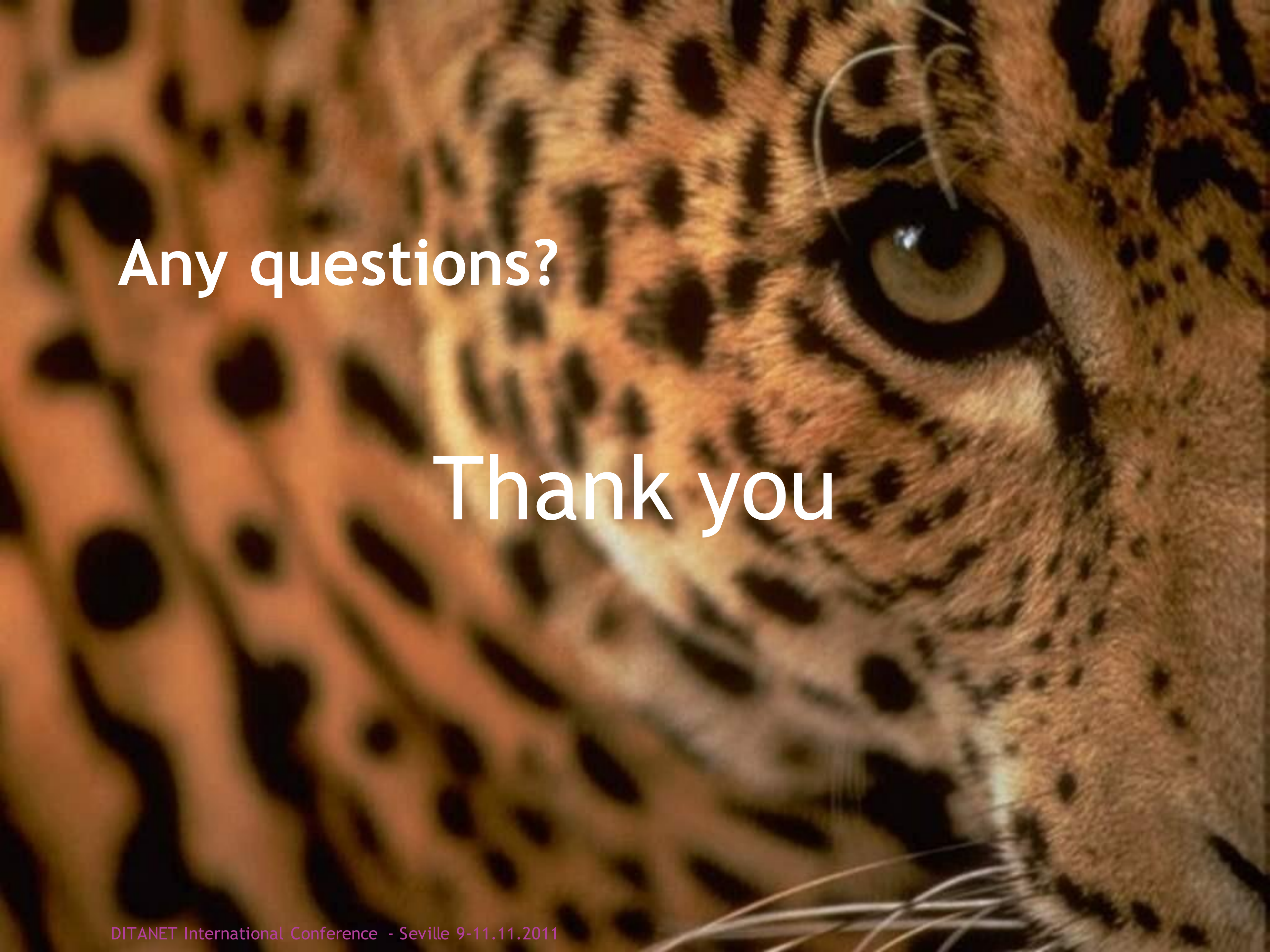

Any questions?

Thank you